





# Beryllium-centred C–H activation of benzene†

 Kyle G. Pearce,  Michael S. Hill \* and Mary F. Mahon

 Cite this: *Chem. Commun.*, 2023, 59, 1453

 Received 8th December 2022,  
 Accepted 5th January 2023

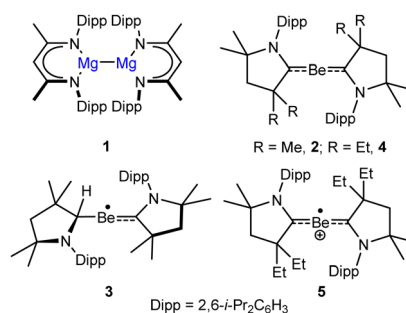
DOI: 10.1039/d2cc06702a

rsc.li/chemcomm

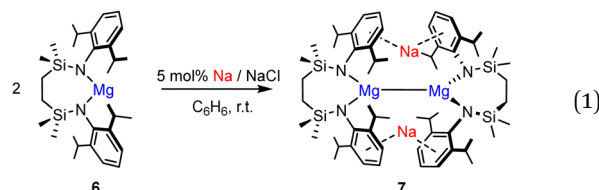
Reaction of  $\text{BeCl}_2$  with the dilithium diamide,  $\{[\text{SiN}^{\text{Dipp}}]\text{Li}_2\}$  ( $\{[\text{SiN}^{\text{Dipp}}] = (\text{CH}_2\text{SiMe}_2\text{NDipp})_2\}$ ), provides the dimeric chloroberyllate,  $\{[\text{SiN}^{\text{Dipp}}\text{BeCl}]\text{Li}_2\}$ , en route to the 2-coordinate beryllium amide,  $[\text{SiN}^{\text{Dipp}}\text{Be}]$ . Lithium or sodium reduction of  $[\text{SiN}^{\text{Dipp}}\text{Be}]$  in benzene, provides the relevant organoberyllate products,  $\{[\text{SiN}^{\text{Dipp}}\text{BePh}]\text{M}\}$  ( $\text{M} = \text{Li}$  or  $\text{Na}$ ), via the presumed intermediacy of transient  $\text{Be}(\text{i})$  radicals.

Despite a reputation as the most toxic non-radioactive element, the coordination, bioinorganic and organometallic chemistry of beryllium has begun to attract more concerted attention.<sup>1–3</sup> More specifically, a flurry of reports have invigorated interest in the lower oxidation state chemistry of the lightest alkaline earth element.<sup>4–7</sup> Although the theoretical viability of  $\text{Be}(\text{i})$ – $\text{Be}(\text{i})$ -bonded species analogous to Jones and co-workers' landmark magnesium(*i*) derivatives (*e.g.* **1**)<sup>8,9</sup> is yet to be realised, exploitation of neutral cyclic alkyl(amino)carbene (CAAC) ligands has led to the isolation of several compounds in which a formal oxidation state  $< +2$  may be assigned to the Be atom. The first examples of charge neutral  $\text{Be}(\text{0})$  (**2**) and  $\text{Be}(\text{i})$  (**3**) compound types were provided by Braunschweig and co-workers through the respective potassium and lithium reduction of CAAC adducts of  $\text{BeCl}_2$  and organoberyllium chloride precursors.<sup>10,11</sup> Although the stability of these compounds has been attributed to strong three-centre-two-electron back-bonding between the Be atom and the carbene ligands, recent calculations have argued that the  $\pi$ -acidic properties of CAACs lend an assignment of a more conventional  $\text{Be}^{2+}$  oxidation state.<sup>12</sup> Gilliard's exploitation of the  $\text{Be}(\text{0})$  species **4**, however, as a reducing agent and to access the radical

cation, **5**, highlight the latent reactivity of such species.<sup>13,14</sup>



Related observations by the Gilliard group have implied that the alkali metal reduction of carbene-ligated halides also proceeds through the transient formation of  $\text{Be}(\text{i})$  radicals.<sup>15</sup> Similarly, Jones and co-workers had earlier inferred that a short-lived blue colour produced during Li reduction of  $[(^{\text{Mes}}\text{B-DI})\text{BeI}]$  ( $^{\text{Mes}}\text{BDI} = \text{HC}\{(\text{Me})\text{CN}-\text{C}_6\text{H}_2\text{Me}_3-2,4,6\}_2$ ) was indicative of transient beryllium radical formation.<sup>16</sup> In contrast, our own study of the potassium reduction of  $[(\text{BDI})\text{BeCl}]$  ( $\text{BDI} = \text{HC}\{(\text{Me})\text{CNDipp}\}_2$ ;  $\text{Dipp} = 2,6\text{-di-}i\text{-isopropylphenyl}$ ) provided no evidence for Be-centred reduction. Rather, a mixture of compounds arising from H-atom transfer between two BDI ligands was suggested to indicate a ligand-based reduction step.<sup>17</sup>

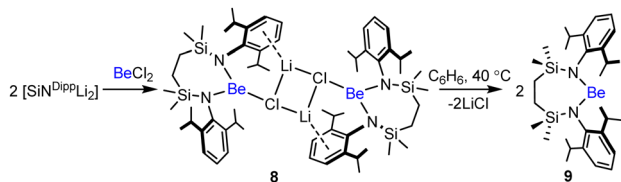


We have recently reported that the  $\text{Mg}(\text{i})$  species,  $\{[\text{SiN}^{\text{Dipp}}]\text{MgNa}\}_2$  (**7**;  $\{[\text{SiN}^{\text{Dipp}}] = (\text{CH}_2\text{SiMe}_2\text{N}(\text{Dipp}))_2\}$ ) may be prepared by sodium reduction of the magnesium(*ii*) precursor **6** (eqn (1)).<sup>18</sup> This approach sought to circumvent conventional salt elimination as a driving force for the reduction and to make deliberate use of the redox-innocence of the  $\{[\text{SiN}^{\text{Dipp}}]\}$

Department of Chemistry, University of Bath, Claverton Down, Bath, BA2 7AY, UK.  
 E-mail: msh27@bath.ac.uk

† Electronic supplementary information (ESI) available: General synthetic experimental details, NMR spectra, X-ray analysis of compounds **8–11**. CCDC 2206119–2206122. For ESI and crystallographic data in CIF or other electronic format see DOI: <https://doi.org/10.1039/d2cc06702a>



Scheme 1 Synthesis of compounds **8** and **9**.

dianion and the robust Na-aryl interactions of **7**. In this contribution we report our initial observations arising from attempts to apply a similar protocol to the isolation of analogous low oxidation state beryllium species.

A reaction of the dilithium diamide,  $[\{\text{SiN}^{\text{Dipp}}\}\text{Li}_2]$ , with  $\text{BeCl}_2$  in hexane provided, after work-up, compound **8** as a colourless solid (Scheme 1). A  $\text{C}_6\text{D}_6$  solution of compound **8** displayed  $^1\text{H}$  and  $^{13}\text{C}$  NMR spectra diagnostic of a  $\text{C}_2$ -symmetric structure. The incorporation of lithium in compound **8** was apparent from the corresponding  $^7\text{Li}$  NMR spectrum ( $\delta_{\text{Li}} -6.6$  ppm) and a broad ( $\omega_{1/2} = 314$  Hz)  $^9\text{Be}$  NMR signal was observed at  $\delta_{\text{Be}} 8.2$  ppm. While tetrahedrally coordinated Be centres have been shown to display chemical shifts in the range  $\delta_{\text{Be}} = -2$  to 8 ppm, this resonance lies to the far low field extreme and the breadth of the signal is more redolent of a lower symmetry environment.<sup>19</sup> Consistent with these solution observations, single crystal X-ray diffraction analysis identified compound **8** as a centrosymmetric lithium diamidochloroberyllate, in which the  $\text{Be1}/\text{Be1}^1$  centres occupy distorted trigonal environments provided by the chelated  $\{\text{SiN}^{\text{Dipp}}\}$  ligands and  $\text{Cl1}/\text{Cl1}^1$  (Fig. S42, ESI<sup>†</sup>). Dimer propagation is achieved by  $\mu_2\text{-Cl-Li-Cl}$  bridging, while each lithium coordination sphere is augmented by  $\eta^6$ -interactions with a single *N*-Dipp substituent of the  $\{\text{SiN}^{\text{Dipp}}\}$  ligands.

The  $^1\text{H}$  and  $^{13}\text{C}$  NMR spectra of **8** did not allow for any discrimination between the *N*-Dipp environments, however, and these solid-state interactions are evidently not retained in solution at room temperature. Further investigation of the solution dynamics of compound **8** was hampered by its apparent conversion on extended storage in  $\text{C}_6\text{D}_6$  to a new species (**9**). This transformation could be accelerated to completion within 16 hours by heating at temperatures  $\geq 40$  °C, a process accompanied by the emergence of a broad ( $\omega_{1/2} = 266$  Hz) resonance in the  $^9\text{Be}$  NMR spectrum at even lower field ( $\delta_{\text{Be}} 11.6$  ppm) than that arising from **8**.

The origin of these observations was resolved by the isolation of colourless single crystals of **9** from benzene suitable for X-ray diffraction analysis (Fig. 1). The solid-state structure of **9** confirmed the elimination of  $\text{LiCl}$  from compound **8** and the production of the initially targeted two-coordinate beryllium analogue of compound **6**. Structurally characterised examples of two-coordinate amidoberyllium monomers are limited to  $[\text{Be}\{\text{N}(\text{SiMe}_3)_2\}_2]$  and 2,6-Mes<sub>2</sub>-C<sub>6</sub>H<sub>3</sub>BeN(SiMe<sub>3</sub>)<sub>2</sub>.<sup>20,21</sup> The more directly comparable homoleptic diamide displayed effectively identical Be–N bond lengths [1.525(2), 1.519(2) Å] to those of compound **9** [N1–Be1 1.515(2), N2–Be1 1.519(2) Å]. In contrast to the almost linear coordination geometry at Be in

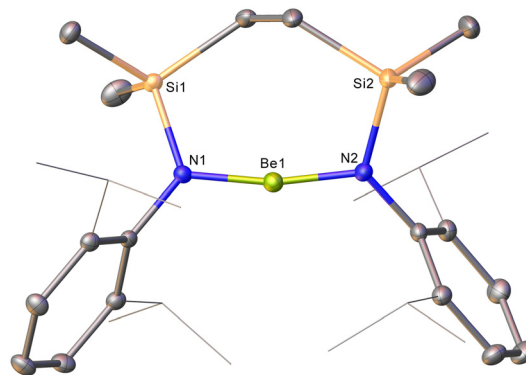


Fig. 1 Displacement ellipsoid (30% probability) plot of compound **9**. Hydrogen atoms are removed and silylmethyl and isopropyl Dipp substituents are shown as wireframe for clarity. Selected bond lengths (Å) and angles (°): N1–Be1 1.515(2), N2–Be1 1.519(2), N1–Be1–N2 168.49(15).

$[\text{Be}\{\text{N}(\text{SiMe}_3)_2\}_2]$  [N1–Be1–N2 178.73(16)°], however, the amide donors of **9** are perturbed to subtend a more acute angle of 168.49(15)°. While we attribute this contrast to the greater constraints placed on the local geometry at beryllium by the seven-membered chelate structure of **9**, it is notable that this angle is still significantly more obtuse than the N–Mg–N angles observed in either of the previously reported structures of the analogous magnesium derivative **6**.<sup>18</sup> In these cases, the coordination spheres of the Mg atoms were augmented by dihapto interactions with a molecule of either benzene [N–Mg–N 132.52(10)°] or toluene [133.92(11)°] solvent, which are, in turn, facilitated by the longer Mg–N bonds [*ca.* 1.95 Å]. On this basis, therefore, the  $\{\text{SiN}^{\text{Dipp}}\}$  ligand of **9** may be assessed to provide significantly greater steric encumbrance of the beryllium atom of **9** than the magnesium centre of its heavier group 2 congener.

A likely consequence of this enhanced kinetic protection was made apparent by initial attempts to effect the sodium reduction of **9** under the reaction conditions applied to the synthesis of compound **7** (eqn (1)). Although the formation of **7** was facile and proceeded smoothly at room temperature, no discernible changes could be observed to the resultant  $^1\text{H}$  NMR spectrum when a  $\text{C}_6\text{D}_6$  solution of **9** was reacted with an excess of 5 wt% Na/NaCl under similar conditions.<sup>22</sup> Further assessment after heating at 100 °C, however, evidenced the generation of multiple new species, albeit the presence of two predominant compounds was characterised by the emergence of new multiplet *isopropyl* methine signals at  $\delta_{\text{H}} 3.90$  and 4.40 ppm. Although the chemical shift ( $\delta_{\text{Be}} = 11.8$  ppm) of the corresponding  $^9\text{Be}$  NMR spectrum was only marginally different to that of **8**, the additional broadening incurred ( $\omega_{1/2} = 327$  Hz) was consistent with a further adjustment to the group 2 element symmetry. Filtration of the resultant solution after two days under these conditions and slow evaporation of the reaction solvent provided a mixture of materials comprising a small but significant quantity of colourless single crystals of compound **10-d** that were suitable for X-ray diffraction analysis (Fig. 2).

Compound **10-d** is a sodium diamidophenylberyllate resulting from the apparent activation of a C–D bond of  $\text{C}_6\text{D}_6$



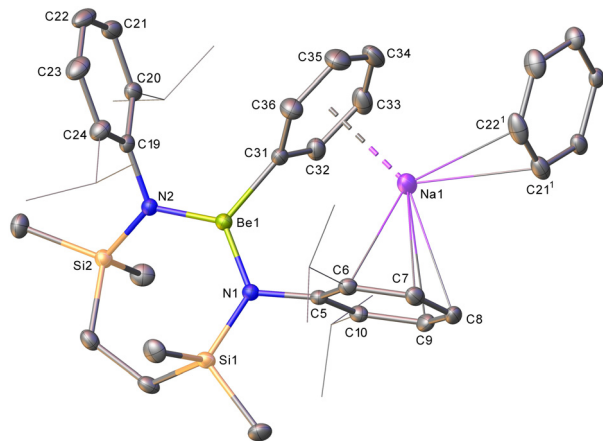
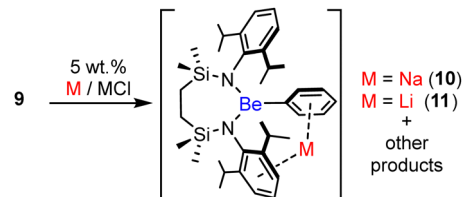


Fig. 2 Displacement ellipsoid (30% probability) plot of compound **10-d**. Hydrogen atoms are removed, and *isopropyl* Dipp substituents are shown as wireframe for clarity. Selected bond lengths (Å) and angles (°): N1–Be1 1.633(4), N2–Be1 1.633(4), C31–Be1 1.779(4), N1–Be1–C31 118.2(2), N2–Be1–N1 125.1(2), N2–Be1–C31 116.6(2). Symmetry operators to generate primed (<sup>1</sup>) atoms,  $1/2 + x, 1 - y, +z$ .



Scheme 2 Synthesis of compounds **10** and **11**.

(Scheme 2). Like those of **8**, the Be atoms occupy distorted trigonal coordination environments while the sodium cations are encapsulated by the C5-containing Dipp group of the Be-chelating  $\{\text{SiN}^{\text{Dipp}}\}$  dianion and the phenyl substituent. Despite these interactions, the Be–*C<sub>ipso</sub>* distance [C31–Be1 1.779(4) Å] is only marginally elongated in comparison to those observed [*ca.* 1.75 Å] in other 3-coordinate and terminally-bonded phenylberyllium derivatives.<sup>23–26</sup> The respective Na-to-centroid distances [2.566, 2.449 Å] are also typical of such polyhaptic Na–arene interactions,<sup>27</sup> while further  $\eta^2$  contacts [Na1–C21<sup>1</sup> 2.783(4), Na1–C22<sup>1</sup> 2.825(4) Å] to an adjacent *N*-Dipp substituent dictate that **10** describes a 1-dimensional polymer propagated along the crystallographic *a*-axis.

The  $\text{C}_6\text{D}_6$  solvent was confirmed as the source of the phenyl substituent of compound **10-d** by performance of an analogous reaction in  $\text{C}_6\text{H}_6$ . Although it was again not possible to isolate a pure bulk sample of **10-h**, its generation was apparent in the mixture of products from two mutually coupled multiplet resonances in the resultant  $^1\text{H}$  NMR spectrum at  $\delta$  6.35 and 6.20 ppm. These signals, absent from the reaction performed in perdeutero solvent, presented a 2 : 1 ratio by relative integration and are, thus, assigned as the respective *m*- and *p*- $\text{C}_6\text{H}_5$  environments of the phenylberyllate unit. This supposition was confirmed by X-ray analysis of a single crystal of **10-h**, which provided identical unit cell parameters to those of **10-d**.

Extension of this reduction chemistry to a reaction performed between **9** and 5 wt% Li/LiCl in  $\text{C}_6\text{D}_6$  heated at 100 °C for 5 days also yielded a mixture of products. The resultant  $^7\text{Li}$  NMR spectrum presented a multiplicity of signals indicative of at least four well discriminated environments, and across a range of chemical shifts between  $\delta_{\text{Li}}$  *ca.* –0.4 and –11.9 ppm. Crystallisation by slow evaporation of the reaction mixture and mechanical separation of a single crystal enabled the identification of compound **11** (Fig. S43, ESI<sup>†</sup>).

Compound **11** is a further diamidophenylberyllate derivative resulting from activation of the benzene solvent (Scheme 2). There are two crystallographically independent molecules in the asymmetric unit, which are effectively identical. The smaller lithium cation evidently prevents the formation of the additional intermolecular interactions that are a feature of the structure of compound **10**. The bond lengths and angles about beryllium are otherwise only marginally perturbed across both the lithium and sodium compounds, obviating further necessary comment.

The low specificity of the reactions that provide compounds **10** and **11** precludes any definitive interpretation. Although other cooperative mechanisms derived either from transient Be(0) formation or Lewis acid-assisted benzene reduction are plausible,<sup>28</sup> we have observed no corroborative evidence for such reactivity (see, ESI<sup>†</sup> for a summary of the control experiments performed). The precedent provided by the comparable magnesium chemistry shown in Scheme 1, therefore, leads us to suggest that the formation of **10** and **11** is a common consequence of the generation of transient beryllium(i) radicals. The formation of diamagnetic Mg–Mg bonded compounds exemplified by **1** and **7** is presumed to occur *via* the dimerisation of transient Mg(i) radical intermediates. Harder and co-workers have shown that a radical species may be effectively trapped by alkali metal reduction of an amidinato magnesium iodide in the presence of CAAC under solid-state (ball milling) conditions.<sup>29</sup> Similar reduction of highly sterically encumbered  $\beta$ -diketiminato magnesium iodides, but performed in benzene and in the presence of *N,N,N',N'*-tetramethylethylenediamine, has yielded binuclear complexes with bridging antiaromatic  $[\text{C}_6\text{H}_6]^{2-}$  dianions. These latter species themselves decompose when heated to provide a mixture of phenyl- and hydridomagnesium derivatives.<sup>30</sup> Jones, Maron and co-workers have also reported that Mg(i) radical formation is induced by photoactivation of the Mg–Mg bonds of compound **1** and related variants.<sup>31</sup> Whereas initial  $[\text{C}_6\text{H}_6]^{2-}$  dianion formation was again observed in benzene solution, UV (370 nm) or blue (456 nm) light-induced photolysis in either toluene or xylene promoted regio- and chemo-selective CH bond activation, and generation of the relevant  $\beta$ -diketiminato magnesium-aryl and magnesium hydride derivatives. Computational studies suggested that benzene reduction is mediated *via* marginally preferential complexation to an initially generated triplet  $\text{Mg} \cdot \cdot \text{Mg}$  ‘ $\sigma$ -bonded’ complex. In contrast, C–H activation of the bulkier arene substrates necessitates dissociation into two doublet (BDI)Mg(i) radical intermediates, albeit again *via* an initial arene dearomatisation step.



Our previous report of compound **7** has highlighted its significantly elongated Mg–Mg bond ( $>3.2$  Å) resulting from a combination of the bulky {SiN<sup>DiPP</sup>} ligands and the separation imposed by the bridging sodium cations necessary to maintain overall charge balance.<sup>18</sup> In the current case, therefore, we suggest that the enhanced steric protection provided to beryllium by the {SiN<sup>DiPP</sup>} ligand in **9** is sufficient to prevent Be–Be bond formation and enable a cascade of Be(I) radical reactivity redolent of the Mg(I) photochemistry deduced by Jones and Maron.

The identification of compounds **10** and **11** provides circumstantial evidence for this latter supposition. Completely analogous behaviour, however, also necessitates hydridoberyllate formation. Although the presence of such species remains to be authenticated, we observe that molecular beryllium hydrides are highly reactive in their own right and have been demonstrated as prone to a variety of inter- and intramolecular C–X bond activation processes.<sup>32–34</sup> In mitigation of our hypothesis, therefore, and taking into account the necessarily harsh thermal conditions necessary for the generation of **10** and **11**, we suggest that the multiplicity of additional species observed alongside both phenylberyllium derivatives is a likely reflection of similar onward Be–H-derived reactivity. We are continuing to explore these possibilities and their extension to alternative group 2 elements and bond activation processes, particularly through variation of the steric demands and structure of the supporting diamide ligand.<sup>35</sup>

KGP performed the synthesis and characterisation of the new compounds reported. MSH conceptualised the study and finalised the manuscript for submission, while MFM finalised the X-ray diffraction analyses for publication.

We acknowledge financial support from the EPSRC (research grant EP/R020752/1).

## Conflicts of interest

There are no conflicts to declare.

## Notes and references

- 1 D. Naglav, M. R. Buchner, G. Bendt, F. Kraus and S. Schulz, *Angew. Chem., Int. Ed.*, 2016, **55**, 10562–10576.
- 2 M. R. Buchner, *Chem. – Eur. J.*, 2019, **25**, 12018–12036.
- 3 M. R. Buchner, *Chem. Commun.*, 2020, **56**, 8895–8907.
- 4 C. Jones, *Commun. Chem.*, 2020, **3**, 159.
- 5 B. Rösch and S. Harder, *Chem. Commun.*, 2021, **57**, 9354–9365.
- 6 L. A. Freeman, J. E. Walley and R. J. Gilliard, *Nat. Synth.*, 2022, **1**, 439–448.
- 7 J. E. Walley and R. J. Gilliard Jr, Recent Adventures in Beryllium Chemistry, in *Encyclopedia of Inorganic and Bioinorganic Chemistry*, 2021, pp. 1–1410, DOI: [10.1002/9781119951438.eibc2788](https://doi.org/10.1002/9781119951438.eibc2788).
- 8 S. P. Green, C. Jones and A. Stasch, *Science*, 2007, **318**, 1754–1757.
- 9 S. A. Couchman, N. Holzmann, G. Frenking, D. J. D. Wilson and J. L. Dutton, *Dalton Trans.*, 2013, **42**, 11375–11384.
- 10 M. Arrowsmith, H. Braunschweig, M. A. Celik, T. Dellermann, R. D. Dewhurst, W. C. Ewing, K. Hammond, T. Kramer, I. Krummenacher, J. Mies, K. Radacki and J. K. Schuster, *Nat. Chem.*, 2016, **8**, 890–894.
- 11 C. Czernetzki, M. Arrowsmith, F. Fantuzzi, A. Gartner, T. Troster, I. Krummenacher, F. Schorr and H. Braunschweig, *Angew. Chem., Int. Ed.*, 2021, **60**, 20776–20780.
- 12 M. Gimferrer, S. Danes, E. Vos, C. B. Yildiz, I. Corral, A. Jana, P. Salvador and D. M. Andrada, *Chem. Sci.*, 2022, **13**, 6583–6591.
- 13 G. C. Wang, L. A. Freeman, D. A. Dickie, R. Mokrai, Z. Benko and R. J. Gilliard, *Chem. – Eur. J.*, 2019, **25**, 4335–4339.
- 14 G. C. Wang, J. E. Walley, D. A. Dickie, S. Pan, G. Frenking and R. J. Gilliard, *J. Am. Chem. Soc.*, 2020, **142**, 4560–4564.
- 15 L. A. Freeman, J. E. Walley, A. D. Obi, G. C. Wang, D. A. Dickie, A. Molino, D. J. D. Wilson and R. J. Gilliard, *Inorg. Chem.*, 2019, **58**, 10554–10568.
- 16 S. J. Bonyhady, C. Jones, S. Nembenna, A. Stasch, A. J. Edwards and G. J. McIntyre, *Chem. – Eur. J.*, 2010, **16**, 938–955.
- 17 M. Arrowsmith, M. S. Hill, G. Kociok-Köhn, D. J. MacDougall, M. F. Mahon and I. Mallo, *Inorg. Chem.*, 2012, **51**, 13408–13418.
- 18 H. Y. Liu, R. J. Schwamm, S. E. Neale, M. S. Hill, C. L. McMullin and M. F. Mahon, *J. Am. Chem. Soc.*, 2021, **143**, 17851–17856.
- 19 J. K. Buchanan and P. G. Plieger, *Z. Naturforsch., B: J. Chem. Sci.*, 2020, **75**, 459–472.
- 20 D. Naglav, A. Neumann, D. Blaser, C. Wolper, R. Haack, G. Jansen and S. Schulz, *Chem. Commun.*, 2015, **51**, 3889–3891.
- 21 M. Niemeyer and P. P. Power, *Inorg. Chem.*, 1997, **36**, 4688–4696.
- 22 J. Hicks, M. Juckel, A. Paparo, D. Dange and C. Jones, *Organometallics*, 2018, **37**, 4810–4813.
- 23 J. Gottfriedsen and S. Blaurock, *Organometallics*, 2006, **25**, 3784–3786.
- 24 M. Müller and M. R. Buchner, *Chem. – Eur. J.*, 2020, **26**, 9915–9922.
- 25 L. R. Thomas-Hargreaves, M. Muller, N. Spang, S. I. Ivlev and M. R. Buchner, *Organometallics*, 2021, **40**, 3797–3807.
- 26 L. R. Thomas-Hargreaves, C. Berthold, W. Augustinov, M. Muller, S. I. Ivlev and M. R. Buchner, *Chem. – Eur. J.*, 2022, **28**, e202200851.
- 27 J. D. Smith, *Adv. Organometal. Chem.*, 1999, **43**, 267–348.
- 28 For example mixtures of Be(0) and alkali metal have been shown to reduce ammonia; M. Müller and M. R. Buchner, *Z. Naturforsch., B: J. Chem. Sci.*, 2020, **75**, 483–489.
- 29 D. Jedrzkiewicz, J. Mai, J. Langer, Z. Mathe, N. Patel, S. DeBeer and S. Harder, *Angew. Chem., Int. Ed.*, 2022, **61**, e202200511.
- 30 T. X. Gentner, B. Rosch, G. Ballmann, J. Langer, H. Elsen and S. Harder, *Angew. Chem., Int. Ed.*, 2019, **58**, 607–611.
- 31 D. D. L. Jones, I. Douair, L. Maron and C. Jones, *Angew. Chem., Int. Ed.*, 2021, **60**, 7087–7092.
- 32 M. Arrowsmith, M. S. Hill, G. Kociok-Köhn, D. J. MacDougall and M. F. Mahon, *Angew. Chem., Int. Ed.*, 2012, **51**, 2098–2100.
- 33 M. Arrowsmith, M. S. Hill and G. Kociok-Köhn, *Organometallics*, 2015, **34**, 653–662.
- 34 K. J. Iversen, D. J. D. Wilson and J. L. Dutton, *Dalton Trans.*, 2014, **43**, 12820–12823.
- 35 **Note added in proof:** Hicks and co-workers have very recently reported that similar reduction of magnesium and calcium diamides with KC<sub>8</sub> in toluene gives rise to the relevant potassium hydrido-magnesiates and -calcates derivatives. In these cases, the origin of the hydride ligands was traced primarily to the arene solvent and the reaction was similarly attributed to the likely formation of short lived magnesium and calcium radical intermediates. See, J. S. McMullen, R. Huo, P. Vasko, A. J. Edwards and J. Hicks, *Angew. Chem. Int. Ed.*, 2023, **62**, e202215218.

